Characterization of self-similarity properties of turbulence in magnetized plasmas

A. Scipioni,[1] P. Rischette,[1,a)] G. Bonhomme,[1] and P. Devynck[2]
[1]*LPMIA, UMR 7040 CNRS-Nancy Université, BP 239, F-54506 Vandoeuvre-lès-Nancy Cedex, France*
[2]*DRFC, Association EURATOM-CEA, CEN Cadarache, F-13108 Saint-Paul lez Durance, France*

(Received 2 January 2008; accepted 3 October 2008; published online 7 November 2008)

The understanding of turbulence in magnetized plasmas and its role in the cross field transport is still greatly incomplete. Several previous works reported on evidences of long-time correlations compatible with an avalanche-type of radial transport. Persistence properties in time records have been deduced from high values of the Hurst exponent obtained with the rescaled range R/S analysis applied to experimental probe data acquired in the edge of tokamaks. In this paper the limitations of this R/S method, in particular when applied to signals having mixed statistics are investigated, and the great advantages of the wavelets decomposition as a tool to characterize the self-similarity properties of experimental signals are highlighted. Furthermore the analysis of modified simulated fractional Brownian motions (fBm) and fractional Gaussian noises (fGn) allows us to discuss the relationship between high values of the Hurst exponent and long range correlations. It is shown that for such simulated signals with mixed statistics persistence at large time scales can still reflect the self-similarity properties of the original fBm and do not imply the existence of long range correlations, which are destroyed. It is thus questionable to assert the existence of long range correlations for experimental signals with non-Gaussian and mixed statistics just from high values of the Hurst exponent. © *2008 American Institute of Physics*. [DOI: 10.1063/1.3006075]

I. INTRODUCTION

The understanding of the nature of turbulence in magnetized plasmas and its role in the cross-field transport is a problem still under study. For example, for the edge turbulence measured in tokamaks, different models or concepts are at the moment discussed. There are models relying on avalanche processes, diffusive ones, local or nonlocal. The validity of models based on self-organized criticality (SOC) (Ref. 1) predicting long range correlations is still in debate. The interpretation and hypotheses which are discussed, mostly rely on the analysis of experimental signals. The R/S analysis[2] is in general used to characterize the self-similarity properties of experimental time series through the calculation of the Hurst parameter. Several previous works[3] have reported analyses performed on experimental data concluding that high H values measured at long time scales was implying the existence of long-range correlations compatible with an avalanche-type of transport.

Our study aims at clarifying the debate on the link between high values of H and the existence of long range correlations. To this end in Sec. II we first give a short summary of the basic concepts and recall the main properties of a fractional Brownian motion (fBm) and a fractional Gaussian noise (fGn) which are the basic models for a self-similar process.[4] In Sec. III we will investigate the limitations of the R/S statistics in determining the Hurst exponent which characterizes the self-affine properties of a time series. Then in Sec. IV we will highlight the great advantages of wavelets as a tool to characterize the self-similarity properties of experimental signals and show that the fractal character of the signal, which is related to a power-law scaling in the spectral domain, can be characterized through the use of discrete as well as continuous wavelets.[5,6]

These tools will be then applied to experimental data, and the results obtained from typical time records from different experiments will be discussed in Sec. V.

In the last section we will try to investigate the surprising relationship observed between long time and short time behaviors for signal with mixed statistics. Our approach is based on numerical simulations of modified fractional Brownian motions.[7,8] We have made use of a similar procedure as Wang *et al.*[9] to generate scrambled data. Indeed they found with the help of a block shuffling procedure the *a priori* surprising result that the destruction of correlations was not modifying the high values of H obtained at long times with the R/S statistics. Their results were later discussed carefully by Gilmore *et al.*[10] Our goal is rather to try to understand the particular mixing of self-similar statistics generally observed in experimental probe data acquired in the scrape-off-layer (SOL) of tokamaks.

II. SELF-SIMILARITY, THE HURST PARAMETER, AND LONG RANGE CORRELATIONS

Extended and detailed discussions of the basic concepts for self-similar and long memory processes can be found in the books by Beran[11] and Wornell;[12] we just give a summary here.

A stochastic process $X(t)$ is statistically self-similar, with parameter (Hurst exponent) H, if its statistics is scale-invariant, i.e., it obeys for any real $a>0$ the scaling relation

a)Permanent address: CReA/MAS'Air, BA701, F-13661 Salon air, France.

 © 2008 American Institute of Physics

Downloaded 08 Nov 2008 to 194.214.217.17. Redistribution subject to ASCE license or copyright; see http://pop.aip.org/pop/copyright.jsp

$$X(t) \overset{d}{=} a^{-H} X(at), \tag{1}$$

where $\overset{d}{=}$ means equality in a statistical sense. If we restrict to Gaussian processes or to wide-sense self-similar processes the equality may be equivalently expressed in terms of second-order statistics, i.e., mean and covariance functions, as

$$E[X(t)] = a^{-H} E[X(at)], \tag{2a}$$

$$E[X(t)X(t')] = a^{-2H} E[X(at)X(at')]. \tag{2b}$$

Most physical processes that exhibit self-similarity are nonstationary. For example the Brownian motion is statistically self-similar with $H=1/2$, but has a stationary derivative, i.e., the zero-mean, white Gaussian noise. This process whose autocorrelation function is a δ–function is also self-similar with parameter $H=-1/2$ (see below).

The most important class of models for such processes are the so-called $1/f$ processes. The $1/f$ family of statistically self-similar stochastic processes are defined as processes having power spectra obeying a power-law relationship of the form

$$S_X(\omega) \sim \frac{\sigma_X^2}{|\omega|^\beta}, \tag{3}$$

where the spectral parameter β is related to H according to $\beta=2H+1$. $\beta \geqslant 1$ corresponds to processes having predominance of low-frequency energy and inherent nonstationarity. For $\beta<1$ the spectrum reflects on contrary a preponderance of high-frequency energy.

From the generalized Fourier pair $|\tau|^{\beta-1}/2\Gamma(\beta)\cos(\beta\pi/2) \leftrightarrow 1/|\omega|^\beta$, where $\Gamma(\cdot)$ is the gamma function, valid for $\beta>0$ but $\beta \neq 1,2,3$ it is seen that the autocorrelation function $R_X(\tau)$ associated with the above spectrum for $0<\beta<1$ is characterized by a slow algebraic decay of the form,

$$R_X(\tau) \sim |\tau|^{\beta-1} \tag{4}$$

which is typical for such $1/f$ processes and corresponds indeed to persistent statistical dependence and long range correlation.

The most popular mathematical models for Gaussian $1/f$ processes are the fractional Brownian motion (fBm) and the fractional Gaussian noise (fGn).[4] fBm are nonstationary Gaussian processes and correspond to $1<\beta<3$. The classical Brownian motion is a special case corresponding to $\beta=2$.

A fBm is a self-similar process $X(t) \equiv B_H(t)$, with parameter H, defined in such a way that its corresponding increment process $\Delta X(t;\delta t)$ defined as

$$\Delta X(t;\delta t) = \frac{1}{\delta t}[B_H(t+\delta t) - B_H(t)] \tag{5}$$

is self-similar *and* stationary for every $\delta t>0$. Its autocorrelation function reads[13,14]

$$R_X(t,t') = E[B_H(t) \cdot B_H(t')] = \frac{\sigma_H^2}{2}(|t|^{2H} + |t'|^{2H} - |t-t'|^{2H}), \tag{6}$$

where $\sigma_H^2 = \Gamma(1-2H)\cos(\pi H)/\pi H$. This nonstationary Gaussian process, with variance $E[B_H(t)^2] = \sigma_H^2 |t|^{2H}$, and satisfying (2 and 3) and is obviously self-similar with parameter H.

The normalized increments of a fBm are stationary and self-similar, and have the autocorrelation[12,15]

$$R_{\Delta X}(\tau;\delta t) \equiv E[\Delta X(t;\delta t) \cdot \Delta X(t-\tau;\delta t)] = \frac{\sigma_H^2 \delta t^{2H-2}}{2}\left[\left(\frac{|\tau|}{\delta t}+1\right)^{2H} - 2\left(\frac{|\tau|}{\delta t}\right)^{2H} + \left(\frac{|\tau|}{\delta t}-1\right)^{2H}\right]. \tag{7}$$

At large lags ($|\tau| \gg \delta t$), the autocorrelation is asymptotically given by

$$R_{\Delta X}(\tau) \approx \sigma_H^2 H(2H-1)|\tau|^{2H-2}. \tag{8}$$

The fractional Gaussian noise (fGn) corresponding to the limit $\delta t \to 0$, i.e., $G_H(t) \equiv \lim_{\delta t \to 0} \Delta X(t;\delta t)$, is the generalized derivative of the fBm. This derivative process is stationary and statistically self-similar with parameter $H'=H-1$, i.e., the fGn has zero mean and $R_{G_H}(\tau) = a^{-2H'} R_{G_H}(a\tau)$ [from Eq. (8)].

Flandrin has shown[16] that the associated power spectral density (PSD) might be expressed as

$$S_{G_H}(f) = W_H \cdot |f|^{-(2H-1)}, \tag{9}$$

where $W_H = \sigma^2/2\Gamma(2H+1)\cdot\sin(\pi H)$. By integrating, one can associate a time-averaged power spectral density to the fBm,

$$S_{B_H}(f) \propto |f|^{-(2H+1)}. \tag{10}$$

Relations (9) and (10) clearly correspond to power law spectra. Furthermore the character of the increment process (fGn) depends strongly on the value of H. For $1/2<H<1$ the derivative process exhibits long-term dependence, i.e., persistent correlation structure [according to Eq. (4)]. Indeed H is a measure of the correlation among signal increments in a time series and is related to the lag n autocorrelation coefficient ρ_n, by $\rho_n = 1/2(|n+1|^{2H} - 2|n|^{2H} + |n-1|^{2H})$, which is Eq. (7) applied to a discrete time series ($|\tau|/\delta t = n$).[10,11,15] The well-known Brownian motion corresponds to $H=0.5$, which increment process is a white Gaussian noise with uncorrelated samples. For a fBm H is in the range 0–1 and for $0<H<0.5$ the derivative exhibits persistent anticorrelation.

Fractional Brownian motions are indeed fractals and the Hurst exponent is generically linked to the fractal dimension (Hausdorff dimension) D of the time series of the increments of the signal by the relationship $D=2-H$.[17] This fractal dimension gives a quantitative measure of the roughness of the graph, e.g., for a continuous function one simply gets $D=1$ ($H=1$) and $D=2$ for $H=0$. For a highly correlated process, i.e., nearly deterministic signal, H will thus be close to 1.

Downloaded 08 Nov 2008 to 194.214.217.17. Redistribution subject to ASCE license or copyright; see http://pop.aip.org/pop/copyright.jsp

III. THE *R/S* STATISTICS AND THE HURST EXPONENT

The existence of cross-field avalanches of energy and particles at all spatial scales associated with a SOC behavior of the plasma would imply that the corresponding turbulent fluctuations exhibit persistence at long time scales. One way to quantify the self-similarity and its domain of existence is the use of the R/S statistics (rescaled range statistics)[2] which allows us to determine H. One defines the ratio R/S in the following way: for a time record segment of length n which is a subset of the total time series of length N ($n \leqslant N$), i.e., $\{X_i : i=1,n\}$, the ratio R/S is

$$\frac{R(n)}{S(n)} = \frac{\max(0, W_1, W_2, \ldots, W_n) - \min(0, W_1, W_2, \ldots, W_n)}{\sqrt{S^2(n)}}, \tag{11}$$

where $W_k = X_1 + X_2 + \cdots + X_k - k\bar{X}(n)$, and where $\bar{X}(n)$ and $S^2(n)$ are the mean and variance of the signal, respectively. It can be shown that R/S behaves asymptotically as n^H if the method is applied to raw data X_i having fractional Gaussian noise (fGn) statistics, i.e., a Gaussian stationary stochastic process. H is found to be equal to $1/2$ if the random samples X_i are statistically independent and their probability density function (PDF) has finite variance (white Gaussian noise).[2]

In fact, the R/S statistics has been used intensively to characterize self-affine processes, such as, fBm. In such a case the R/S analysis must be applied to the successive increments of the signal, i.e., to the fGn associated with the signal. This very important point has been already pointed out by Cannon *et al.*[18] and again more recently by Gilmore.[10] In this case H expresses the dependencies or correlation between past and future increments, which for fBm data $B_H(t)$ reads [e.g., from $R_{\Delta X}(-\Delta t;\Delta t) = \sigma_H^2 \Delta t^{2H-2}[2^{2H-1}-1]$ given by Eq. (7)]

$$C(\Delta t) = \langle [B_H(0) - B_H(-\Delta t)] \times [B_H(\Delta t) - B_H(0)] \rangle / \langle B_H(\Delta t)^2 \rangle = 2^{2H-1} - 1. \tag{12}$$

This incremental correlation function is independent of Δt and its sign depend on H. If $H > 1/2$, then $C(\Delta t) > 0$ and this expresses the trend in the fBm at a given time to be followed likely by a similar one (persistence). On the contrary if $H < 1/2$, then $C(\Delta t) < 0$ and there is a tendency for a change in the sign of the next increment (antipersistence).

There is, in this case, a direct relationship between the H parameter given by the R/S statistics and the spectral properties of the time series.[15] The power spectral density (PSD) of the successive increments (fGn) exhibits the power-law scaling $f^{-(2H-1)}$, and the PSD of the signal (fBm) behaves as $f^{-(2H+1)}$ (see Sec. II). Thus, for $H=1/2$, the related power frequency spectra have a slope (in log-log scale) $\beta=0$ for the increments of the signal, and a slope $\beta=2$ for the signal itself.

To summarize, the relationship between H calculated with the R/S method on the increments of the signal (time derivative) and the absolute value β of the slope of the PSD of the signal (in log-log scale) is $\beta = 2H+1$.

It is useful to complete this information by indicating that taking the derivative of the signal modifies the relationship between H and the slope β that becomes $\beta = 2H-1$. This shows the limitations of the R/S statistics which is only able to measure values of H between 0 and 1, corresponding to the exponent β of the related power-law scaling of the PSD being between -1 and $+1$ for the increments of the signal and between 1 and 3 for the signal itself. This is clearly a great drawback when analyzing experimental signals with mixed statistics, making it necessary to apply successively the method to the signal and then to its increments. Another approach without these disadvantages relies on the wavelet-based method.

IV. WAVELETS AND THE HURST EXPONENT

The continuous wavelet transform (CWT) of a function f consists of the decomposition of this function into a sum of elementary wavelets which are built from dilatation and translation from a single mother wavelet ψ. Thus, the continuous wavelet transform of f is defined as[5,15]

$$T_\psi[f](a,b) = \frac{1}{\sqrt{a}} \int_{-\infty}^{\infty} f(x) \bar{\psi}\left(\frac{x-b}{a}\right) dx \tag{13a}$$

$$\propto \langle f, \psi \rangle, \tag{13b}$$

where $\langle \cdot, \cdot \rangle$ means inner product.

The CWT allows any arbitrary choice of scale but is very demanding on computer time. Among the different possible choices, we have chosen the Daubechies mother wavelets. This latter allows us to define a discrete wavelet transform (DWT) for which very powerful algorithms exist, but for which the analysis is limited to scales expressed in octaves.

It has been shown[6,15] that the wavelet transform allows us to characterize the self-affine properties of a time series simply from a log-log plot of the variance of the wavelets coefficients as a function of the scale a. The self-affinity properties of the time series are reflected by the existence of a constant slope of value $2H+1$ on this curve. This is depicted in Figs. 1 and 2 for a simulated classical Brownian motion ($H=0.5$).

Let us examine the reasons why the wavelets offer a very highly suitable tool to study processes with PSD having a power-law scaling.

First, wavelet techniques can be used to generate a stationary, at all scale, self-similar process.[12] Actually $x(t)$ being a self-similar process with parameter H, one can build, by using a CWT, the filtered process $x_a(t) = \mathrm{CWT}\,[x](a,t)$, $t \in \mathbb{R}$, where a is the scale parameter. Its autocovariance function R_{x_a}, reads[19–21]

Downloaded 08 Nov 2008 to 194.214.217.17. Redistribution subject to ASCE license or copyright; see http://pop.aip.org/pop/copyright.jsp

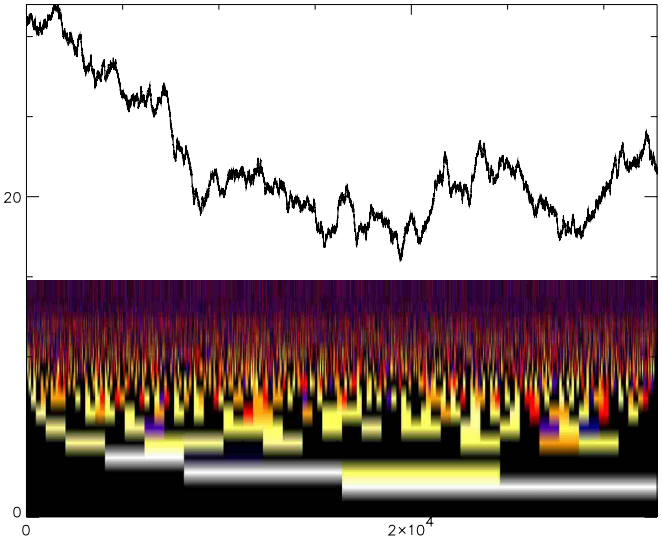

FIG. 1. (Color online) Discrete wavelet transform (DWT): Brownian motion $H=0.5$.

$$R_{x_a} = E[x_a(t)\cdot x_a(t')] \tag{14a}$$

$$= \frac{\sigma^2}{2}\int \psi_{a,t}(u)du \cdot \int |v|^{2H}\psi_{a,t'}(v)dv + \frac{\sigma^2}{2}\int \psi_{a,t'}(v)dv \cdot \int |u|^{2H}\psi_{a,t}(u)du - \sigma^2 a^{2H+1}\int |u|^{2H} s_\psi\left(\frac{t-t'}{a}-u\right)du. \tag{14b}$$

The wavelet having zero mean (i.e., the number of vanishing moments is $M \geqslant 1$, where M is the integer such as $\forall k \in \{0,\cdots,M-1\}$, $\langle t^k, \psi(t)\rangle = 0$), one has

$$R_{x_a} = -\sigma^2 a^{2H+1}\int |u|^{2H} s_\psi\left(\frac{t-t'}{a}-u\right)du. \tag{15}$$

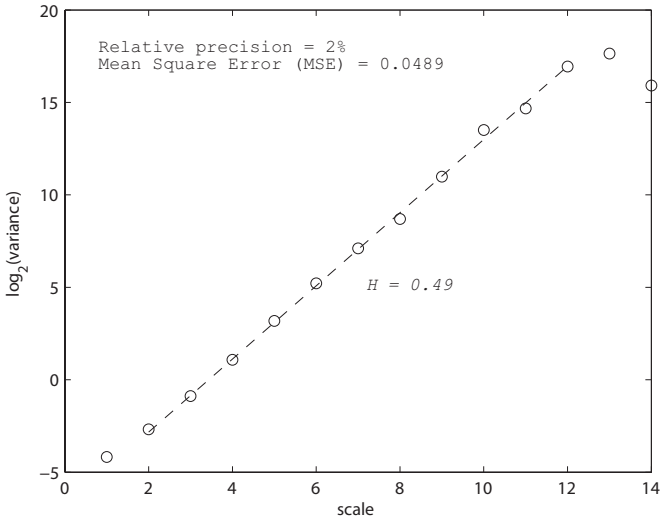

FIG. 2. Hurst parameter from the DWT: Brownian motion $H=0.5$.

As R_{x_a} depends only on the time delay $\tau=t-t'$, x_a is a stationary process. Its PSD is obtained from the Fourier transform of Eq. (15) and behaves as

$$S_{x_a}(f) \propto \sigma^2 |f|^{-(2H+1)} a |\Psi(af)|^2 \tag{16}$$

in the case of a fBm for which $S_{B_H}(f) \propto \sigma^2 |f|^{-(2H+1)}$ [see Eq. (10)].

In this case, the bias (systematic error) of the estimator, i.e., $E[S_{x_a}(f)] - \sigma^2|f|^{-(2H+1)}$ can be obtained from[22–25]

$$E[S_{x_a}(f)] = \sigma^2 |f|^{-(2H+1)} \cdot \underbrace{\left[f_\psi^{(2H+1)} \int |\nu|^{-(2H+1)} \widetilde{\mathcal{RK}}(a,\nu) d\nu \right]}_{(i)}, \tag{17}$$

where f_ψ is the central frequency of the analyzing wavelet, and $\widetilde{\mathcal{RK}}$ is the Fourier transform of the CWT reproducing kernel,[26] with $\mathcal{RK}(a,t;a,t+u) = \langle \psi_{a,t}, \psi_{a,t+u}\rangle = R_{\psi_{a,t}}(u)$ that is a measure of the correlation between two analyzing wavelets. The factor (i) does not depend on the analyzed frequency f and consequently, if a power law exists, the wavelet-based estimator will be able to highlight it in an unbiased way.

Second, let us consider the link between the power-law behavior of the process $x(t)$ and the scale invariance property characteristic of the CWT. This one is based on a scaling operator $\mathcal{S}$,

$$\psi(t) \overset{\mathcal{S}}{\rightarrow} \psi_a(t) = \frac{1}{\sqrt{a}} \cdot \psi\left(\frac{t}{a}\right), \tag{18}$$

where $\psi(t)$ is the mother wavelet and $\psi_a(t)$ is the wavelet analyzing the process at scale a. Thus, the CWT has by construction the scale invariance property. Consequently, the variance $E[x_a(t)^2]$ has necessarily a power-law behavior[19]

$$E[x_a(t)^2] = a^{2H+1} P(H), \tag{19}$$

where $P(H)$ denotes a polynomial function. The estimation of H is obtained from a linear regression in a $\log\{E[x_a(t)^2]\}$ versus $\log a$ representation.

The CWT makes it possible to locate with great precision in the time domain the analyzing unit box on the signal. But the resulting strong redundancy (correlation between coefficients and a very high number of coefficients) implies very long computer time and implementation difficulties.

The discrete wavelet transform (DWT) is a nonredundant transform but performs a spectral analysis only by octaves. On the other hand, an implementation by means of the Mallat algorithm[27] results in a very low computation cost. Its spectral estimator, relying on the energy of the detail coefficients, reads[28]

$$S_{d,x}(j) = \frac{1}{2^{-j}N}\sum_{k=1}^{2^{-j}N} \langle x, \psi_{j,k}\rangle^2, \tag{20}$$

where j is the scale, N the number of points at scale 0, and $\langle x, \psi_{j,k}\rangle$ are the detail coefficients. In the case of a fBm, Eq. (17) providing the bias becomes

Downloaded 08 Nov 2008 to 194.214.217.17. Redistribution subject to ASCE license or copyright; see http://pop.aip.org/pop/copyright.jsp

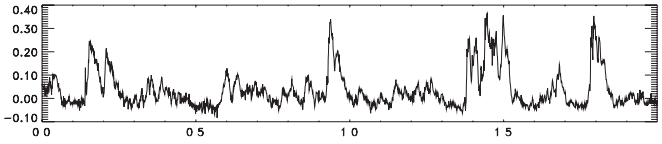

FIG. 3. Experimental data: A subrecord of density fluctuations (Tore-Supra shot #22253).

$$E[S_{d,x}(j)] = \sigma^2 2^{-j(2H+1)} \cdot f_\psi \int |\nu|^{-(2H+1)} |\psi(\nu)|^2 d\nu. \quad (21)$$

Taking into account the respective advantages of the two transforms, the Daubechies wavelets have been chosen for CWT and DWT transforms.

The use of the wavelet-based method to the experimental data is now discussed below.

V. ANALYSIS OF EXPERIMENTAL DATA

First we have used the R/S analysis to characterize self-similarity properties and to calculate the Hurst exponent for Langmuir probe data acquired in the SOL of tokamaks. We discuss here the results obtained from the analysis of two typical signals measured in the Tore Supra[9] and Castor[29,30] tokamaks (Figs. 3 and 4).

A first observation is that the density power spectra show two distinct behaviors at different time scales. Actually the presence of an elbow on the spectrum (Figs. 5 and 6) is indicative of the different statistical properties of the signal at large and small time scales, the breakpoint occurring at a time scale corresponding to the characteristic autocorrelation time, denoted τ_L in all the figures, of the order of 100 μs. Such a mixed statistics is common feature of fluctuations data from SOL turbulence.

Indeed we observe that the experimental signal behaves at small time scales (the slope of the frequency spectrum in log-log scale is $\beta \approx 2$) as a fractional Brownian motion signal. However, at large time scales (corresponding to the low frequency domain with a very weak slope on the spectrum) the behavior is analogous to one of the successive increments of a fractional Brownian motion signal, i.e., a fractional Gaussian noise. As a direct consequence of this observation we have to use the R/S method differently depending on the time scale. The analysis is first performed directly on the signal itself, then on its increments (time derivative of the signal). Each curve R/S shows two distinct regions in agreement with the spectral properties.

The properties at large time scales are deduced from the R/S curve calculated on the signal itself (Figs. 7 and 8). For the Tore-Supra case this curve gives for large time scales a

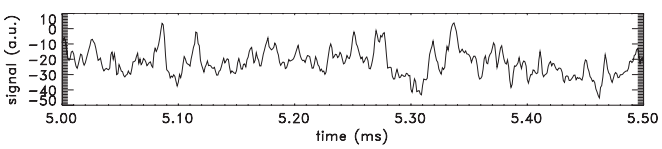

FIG. 4. Experimental data: subrecord of density fluctuations (Castor shot #9525).

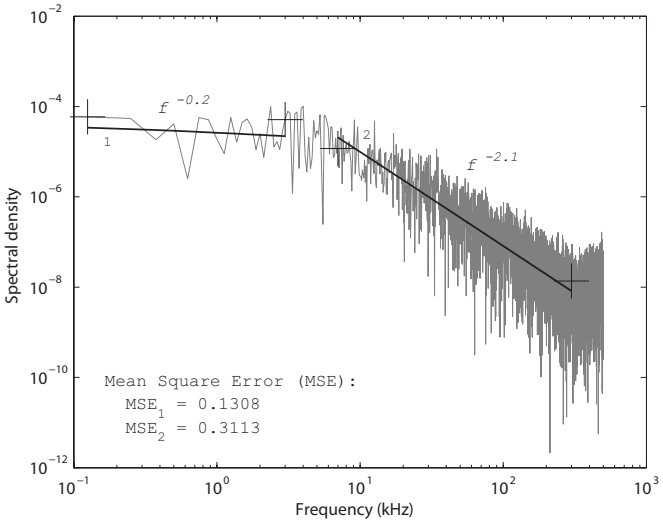

FIG. 5. Tore-Supra shot #22253: power spectral density.

value of $H=0.50$ to which corresponds a power law of the frequency spectrum with $\beta=0$ in the low frequency region, the relationship in this case being $\beta=2H-1$. We can immediately check on the PSD (see Fig. 5) that this relationship is indeed verified. For the Castor time series the R/S curve (Fig. 8) gives $H=0.84$ again in agreement with the $f^{-0.7}$ power-law (see Fig. 6), taking into account the accuracy of the measurement.

As far as the behavior at large time scales is concerned, in most cases we do measure H values larger than 0.5 and such results are in agreement with the ones of Carreras *et al.*,[3] and this would lead us to the same conclusions, namely the existence at large time scales of a self-similar behavior displaying persistency, compatible with transport theories based on the SOC behavior.[1] However, the turbulent signal does not have characteristics of a pure fractional Brownian motion, because it possesses two regions with different self-similar properties and is moreover non-Gaussian. If we look at the properties of the signal at small time scales

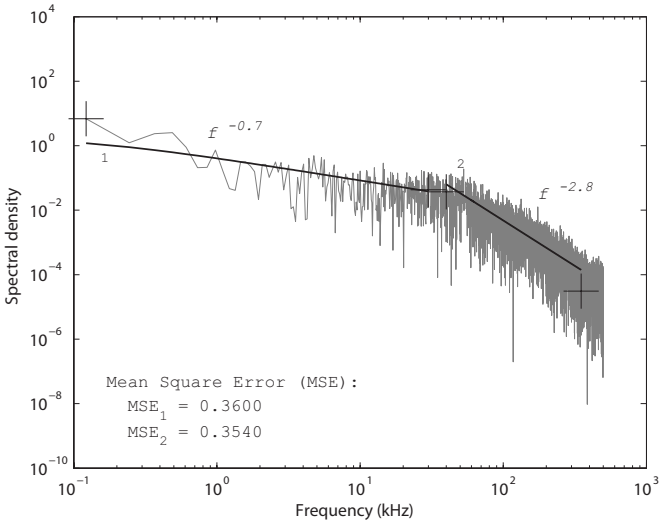

FIG. 6. Castor shot #9525: power spectral density.

Downloaded 08 Nov 2008 to 194.214.217.17. Redistribution subject to ASCE license or copyright; see http://pop.aip.org/pop/copyright.jsp

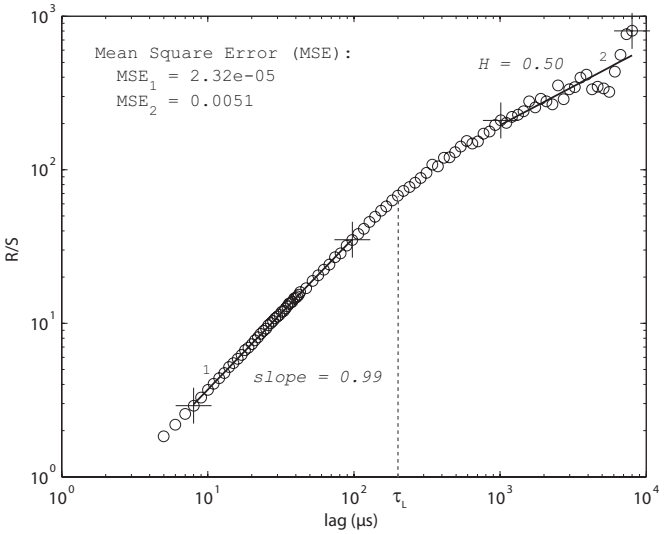

FIG. 7. Tore-Supra shot #22253: R/S on the signal.

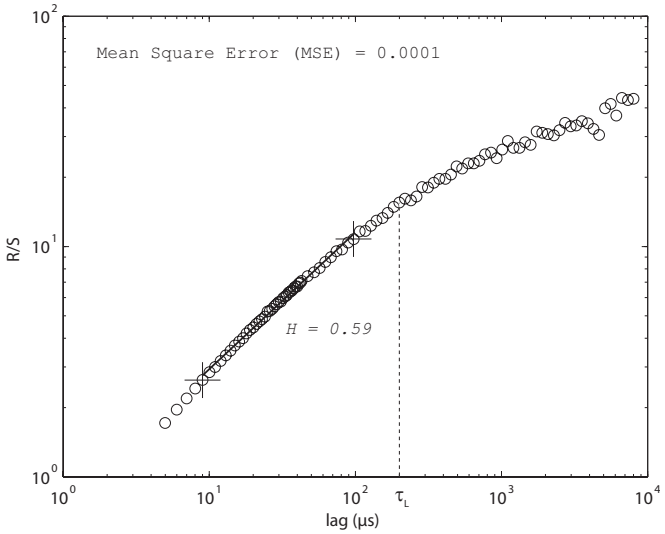

FIG. 9. Tore-Supra shot #22253: R/S on increments of the signal.

by computing the R/S statistics on the time derivative of the signal (Figs. 9 and 10), we obtain from the slope at small time scales a Hurst exponent $H=0.59$ in good agreement with the exponent of the power law of the frequency spectrum $\beta=2.1$ for the Tore-Supra case, the relationship being in this case $\beta=2H+1$, and $H=0.86$ in perfect agreement with the $f^{-2.8}$ power law for the Castor case as well.

Then we take advantage of the ability of a wavelet-based method to pick up at once self-similarity properties at all scales. All the previous results are compared with those obtained by means of a wavelet-based method. The variance plots corresponding to the CWT using Daubechies db2 are shown in Fig. 11 and Fig. 12, respectively. The variance of wavelets coefficients obtained from a discrete transform (using Daubechies db2 as well) is depicted in Fig. 13. Hurst exponents are obtained from a linear regression based on a weighted least squares estimator.[15]

We immediately see that the Hurst exponents obtained with this method are in excellent agreement with the ones obtained by using the R/S method in both frequency domains, i.e., large scales and small scales. Explicitly, for the Tore-Supra case, the obtained values $H=0.53$, and -0.47 (Fig. 11) correspond, respectively, to the power laws $f^{-2.06}$ and $f^{-0.06}$ in good agreement with the experimental spectrum. For the Castor case the obtained values $H=0.82$ and -0.16 (cf. Fig. 13) would give $f^{-2.64}$ and $f^{-0.68}$, respectively, also in very good agreement with the spectrum (Fig. 6).

A decisive advantage of the wavelet-based method is that it makes it possible to obtain directly at all scales the self-similarity properties and the corresponding exponents.

A very surprising result is the unexpected closeness of the H exponents calculated in the two different time or frequency domains. Indeed for all the studied time series one notices that the Hurst exponent characterizing the behavior at small scales is very close to that obtained for large scales (Figs. 7 and 9 and Figs. 8 and 10, respectively). This would correspond, if the temporal series were generated by frac-

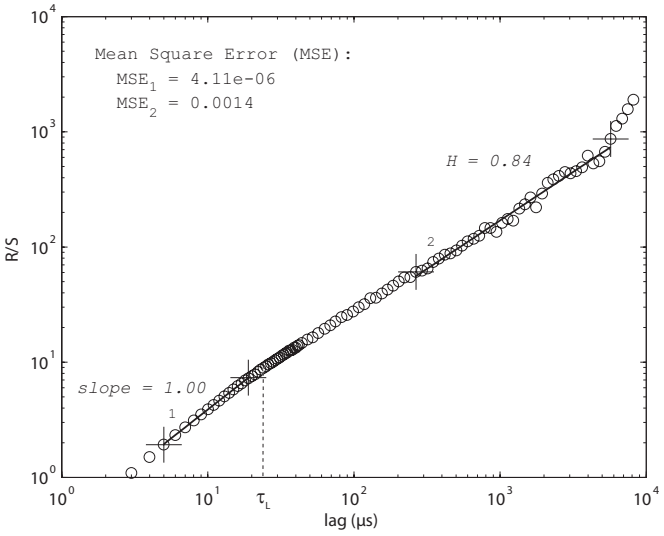

FIG. 8. Castor shot #9525: R/S on signal.

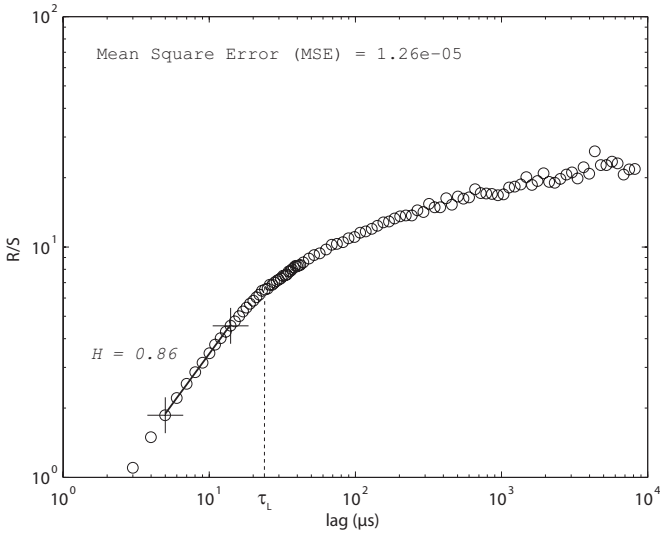

FIG. 10. Castor shot #9525: R/S on increments.

Downloaded 08 Nov 2008 to 194.214.217.17. Redistribution subject to ASCE license or copyright; see http://pop.aip.org/pop/copyright.jsp

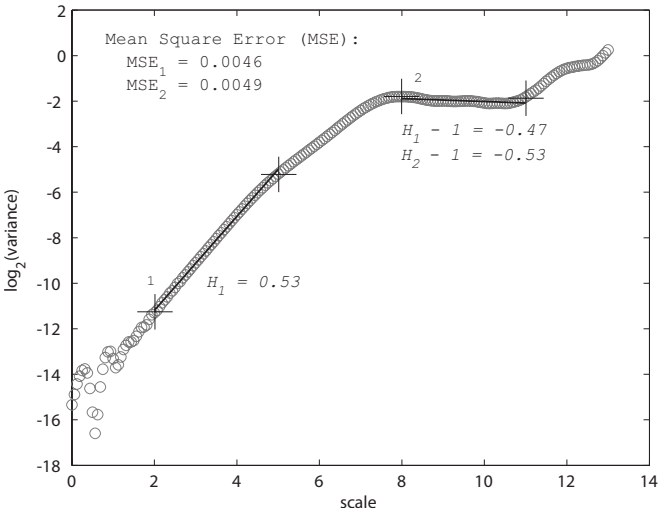

FIG. 11. Hurst parameter from the db2 CWT: Tore-Supra shot #22253.

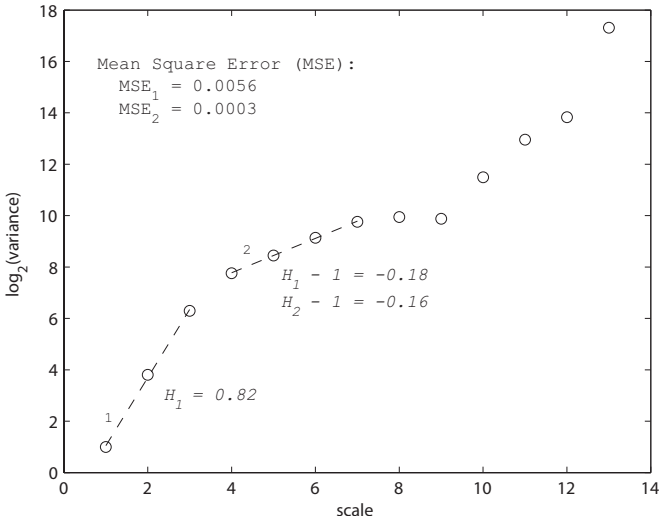

FIG. 13. Hurst parameter from the DWT: Castor shot #9525.

tional Brownian motions, to a large-scale behavior fGn-like, and at small scales fBm-like with very nearby characteristic exponents.

VI. ANALYSIS OF SIMULATED MODIFIED FRACTIONAL BROWNIAN MOTIONS

In the next step of this work, we study modified fractional Brownian motion signals and try to understand the origin of this surprising relationship, and to investigate the link between a high value of the Hurst parameter H, and long-time correlation. To this end we applied the test proposed by the authors of Ref. 9 and discussed carefully later by Gilmore *et al.*[10]

Data from simulated fGn or fBm have been broken into blocks of length M, and the blocks scrambled randomly. The scrambled and unscrambled data were then used to calculate H parameters by using the R/S method and the wavelet techniques as well. The shuffling of blocks of length M should destroy any correlation existing for time scales larger than M.

In the above cited work[10] the test was applied to time series of fGn data broken into blocks of length from $M=10$ to 500 samples and the main result was that indeed M must be very small in order to destroy completely these correlations. The breakpoint lag in the R/S curve reflecting the effect of the randomization of blocks is larger than the expected autocorrelation time.

We have performed the same procedure first on scrambled fGn and compared the results of the R/S analysis and the wavelet-based method. The results we have obtained are in full agreement with Gilmore *et al.* and some examples are depicted in Figs. 14–16. Figure 14 shows the result of the R/S analysis, and in Fig. 15 the results obtained from the discrete wavelet decomposition are depicted. Figure 16 shows for comparison the result obtained with a continuous wavelet transform.

But further we have carried out a similar analysis on broken fBm, which provides a very simple, though a bit crude, model of data with mixed statistics. In the case of

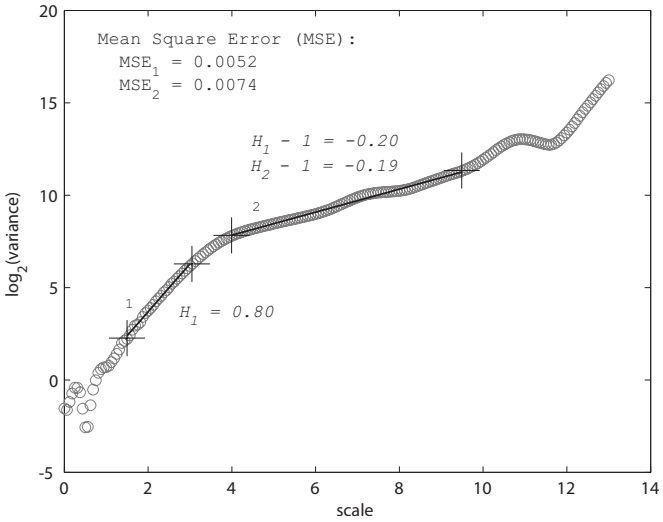

FIG. 12. Hurst parameter from the db2 CWT: Castor shot #9525.

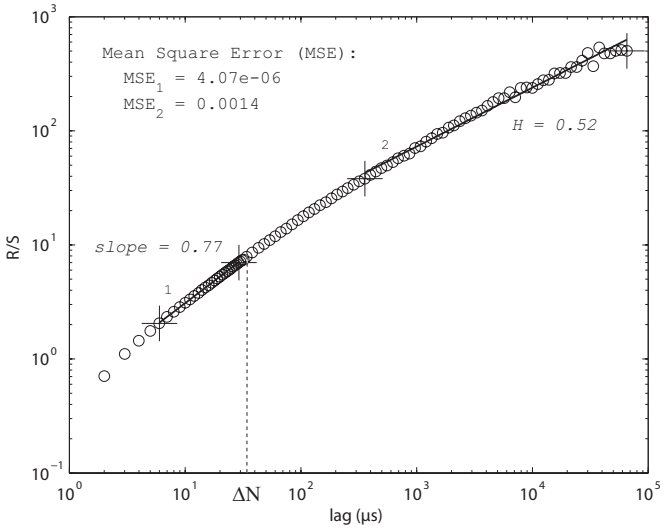

FIG. 14. Scrambled fGn ($H=0.7$, $M=32$): R/S on signal.

Downloaded 08 Nov 2008 to 194.214.217.17. Redistribution subject to ASCE license or copyright; see http://pop.aip.org/pop/copyright.jsp

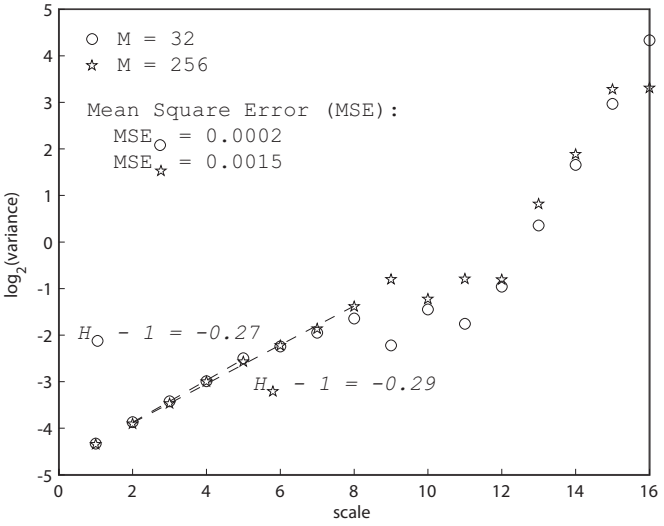

FIG. 15. Scrambled fGn ($H=0.7$, $M=32$ and $M=256$): DWT.

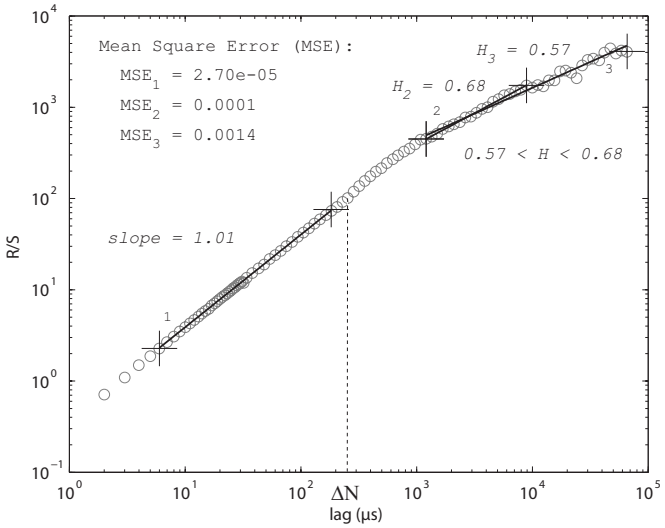

FIG. 17. Scrambled fBm ($H=0.7$, $M=256$): R/S on signal.

short blocks ($M=32$) and when the R/S analysis is applied directly to the signal we get $H\approx 0.5$ at large time lags which corresponds to a classical Brownian motion and in agreement with the destruction of the correlations by the shuffling procedure.

But in the case of larger blocks the results obtained with the R/S method depicted in Figs. 17 and 18 show that we get similar values $H\approx 0.7$, both at small time lags ($H=0.75$ when the analysis is performed on the increments, Fig. 18) and large ones ($0.6\lesssim H\lesssim 0.7$ when the analysis is performed directly on the signal, Fig. 17). These results are also in agreement with the power-law scalings observed on the PSD (Fig. 19). Obviously the high H value measured at large time lags much larger than M cannot be related to the existence of long-time correlations (they have been destroyed) and thus must be entirely determined by the statistics at small time scales.

These results are fully confirmed by the wavelet analysis. Long times series (2^{20} samples) of simulated fBm with $H=0.7$ have been broken into blocks of three different lengths ($M=32,256,2048$) and shuffled. The results obtained by applying a DWT analysis to the scrambled fBm and to its increments are shown in Figs. 20 and 21, respectively. It is clear that the original properties remain not only at very small scales, but also to large scales far beyond the block size.

In order to understand this result we must realize that even if the shuffling procedure does destroy long-time correlations the long-time behavior of a shuffled fBm is not that of a fractional Gaussian noise. The block shuffling procedure creates jumps between the blocks and furthermore each individual block still possess a trend resulting from the initial fBm. This could explain the reason why an R/S analysis performed on the signal at large time scales gives a H value which is in fact a measure of a relic of the self-similarity of the original fBm.

In order to test the validity of this intuition we have applied a detrending procedure to each block. To this purpose we have made use of the so-called Empirical Mode

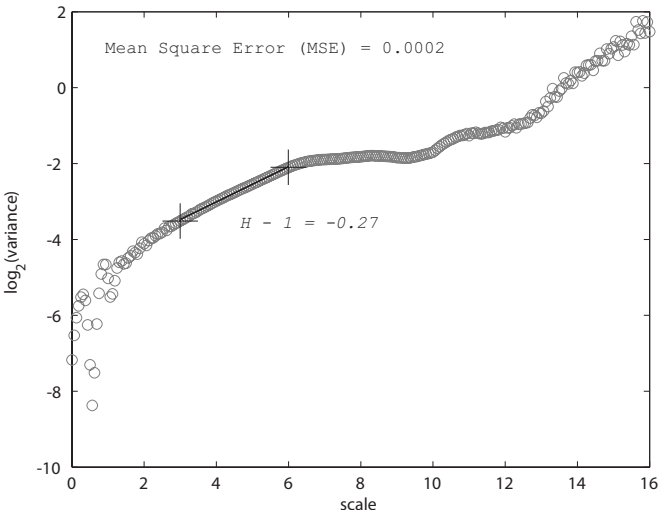

FIG. 16. Scrambled fGn ($H=0.7$, $M=32$): CWT.

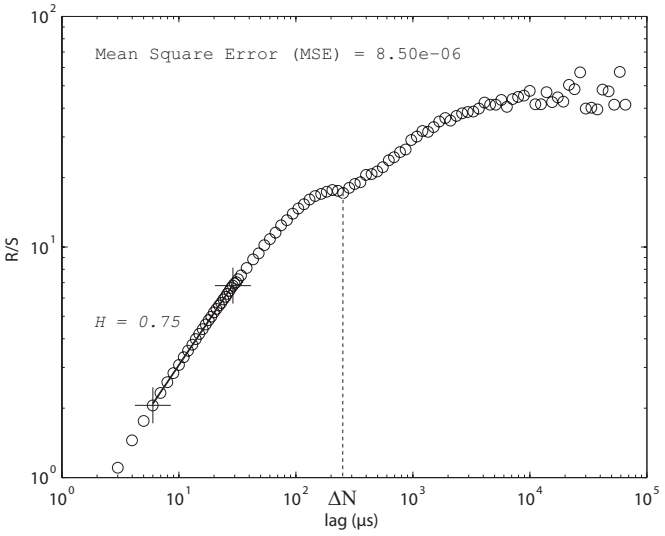

FIG. 18. Scrambled fBm ($H=0.7$, $M=256$): R/S on increments.

Downloaded 08 Nov 2008 to 194.214.217.17. Redistribution subject to ASCE license or copyright; see http://pop.aip.org/pop/copyright.jsp

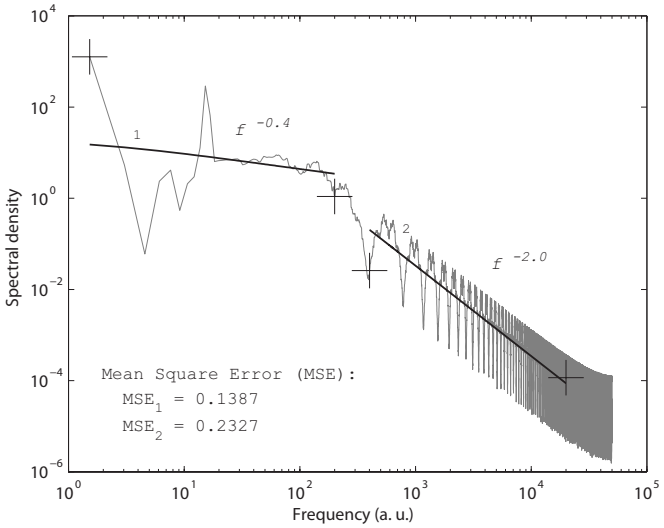

FIG. 19. Scrambled fBm ($H=0.7$, $M=256$): power spectral density.

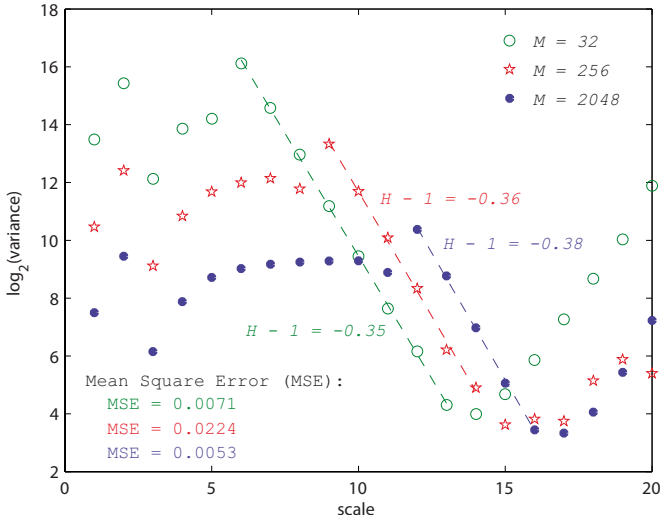

FIG. 21. (Color online) Scrambled fBm ($H=0.7$, $M=2^5$, $M=2^8$, and $M=2^{11}$): DWT on increments.

Decomposition introduced by Huang *et al.*[31] The result is quite clear: the Hurst exponent characterizing the long-time behavior of shuffled fBm consisting of detrended blocks with zero mean is close to 0.5. The result is depicted in Fig. 22. In conclusion by applying a procedure of random shuffling of blocks to simulated fractional Brownian motions we get the result that, for the simulated data, $H>0.5$ measured at large time scales still reflect the original self-similar behavior and gives no evidence at all of long range correlations which do not exist.

VII. DISCUSSION AND CONCLUSIONS

Our first conclusion is that a great care must be taken when using the R/S method to characterize time series with different statistics at long and small time scales. It is indeed the case when analyzing time series of plasma fluctuations data acquired at the edge of tokamaks. The H parameter which characterizes the self-similarity of the signal at small time scales (fBm-like behavior) can be obtained by applying the R/S method on the increments (time derivative) of the signal. On the other hand the properties of the signal at large time scales (fGn-like behavior) could be obtained with the R/S same analysis directly performed on the signal itself.

Then we have shown that using a wavelet decomposition technique, it is possible to deduce the self-similarity properties of the signal at once on all time scales. The Hurst exponents obtained with this method are in excellent agreement with the ones obtained by the using the R/S method. Moreover we have shown that the wavelets method does not have the limitations of the R/S analysis, in the sense that they allow to quantify the self-similarity of signals having arbitrary Hurst exponents.

Numerical simulations performed with modified fractional Gaussian noise and fractional Brownian motion signals (by random shuffling of blocks of length M of data) helped us to understand the results obtained by Wang *et al.*[9]

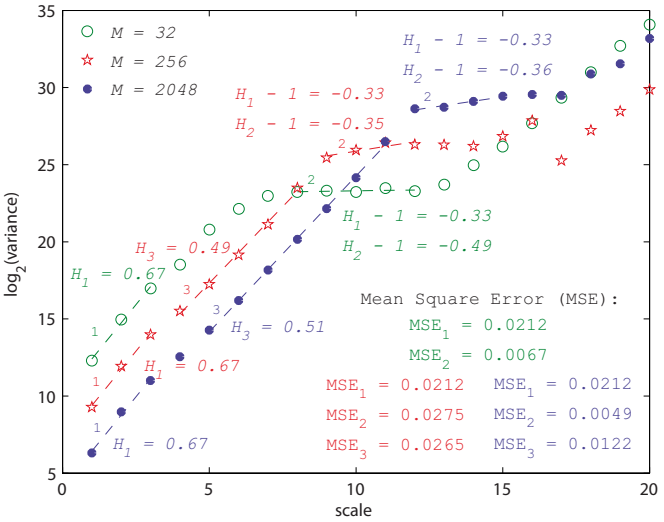

FIG. 20. (Color online) Scrambled fBm ($H=0.7$, $M=2^5$, $M=2^8$ and $M=2^{11}$): DWT on signal.

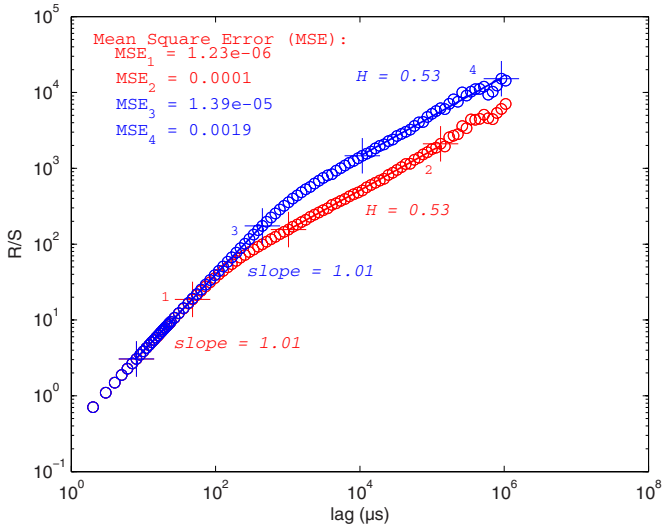

FIG. 22. (Color online) Scrambled fBm after detrending of each block ($H=0.7$, $M=256$, and $M=2048$): R/S on signal.

Downloaded 08 Nov 2008 to 194.214.217.17. Redistribution subject to ASCE license or copyright; see http://pop.aip.org/pop/copyright.jsp

who applied the same shuffling technique to experimental data to test the existence of correlations at large time scales. Our results based on a comparison between R/S and wavelet-based methods are in agreement with the Gilmore *et al.*[10] discussion which was based on the structure function method. Moreover we have shown by applying this test to fBm instead of fGn, that for blocks larger than the autocorrelation time, and in spite of the shuffling process the H value of the original fBm is still present not only at small scales, i.e., smaller than the block size, but also at large scales. The original self-similarity parameter is still contained in the statistics of the jumps between the blocks and their individual trends. In this particular case it originates from the dynamics at small time scale and is in no way connected to the existence of correlations at long time scales. This ultimately provides a clear explanation of the surprising results reported by Wang *et al.*

Of course the experimental time series, although they also exhibit mixed statistics properties are not shuffled fBm. Nevertheless the results we have obtained could open a track to explain the surprising results obtained in different machines, i.e., an unexpected relationship between the H exponents relative to large and small time scales, respectively. At large time scales, the measured H parameter clearly depends on the non Gaussian statistical properties of large amplitude events but of short duration (i.e., bursts). As a result, large values of H can be measured even without any long-range correlation and thus does not imply necessarily the existence of persistency at large time scales and this would put back into question the picture of a radial transport caused by avalanches at all scales.

The important question is to understand the origin of the mixed statistics property of experimental signals, and the relationship between the statistical properties of the intermittent bursts and the self-similarity behavior at small and large time scales. However, it is clear that to this end and with the intention of choosing among the different transport models, analysis of longer time series obtained from synchronous multipoint measurements are needed.

ACKNOWLEDGMENTS

We thank the Castor team in Prague for providing us the Castor data used in this work.

[1] P. Bak, C. Tang, and K. Weisenfeld, Phys. Rev. Lett. **59**, 381 (1987).
[2] J. Feder, *Fractals* (Plenum, New York, 1988), pp. 149–183.
[3] B. A. Carreras, B. P. van Milligen, M. A. Pedrosa, R. Balbin, C. Hidalgo, D. E. Newman, E. Sanchez, M. Frances, I. Garcia-Cortes, J. Bleuel, M. Endler, C. Riccardi, S. Davies, G. F.Matthews, E. Martines, V. Antoni, A. Latten, and T. Klinger, Phys. Plasmas **5**, 3632 (1998).
[4] B. B. Mandelbrot and J. W. van Ness, SIAM Rev. **10**, 422 (1968).
[5] M. Farge, Annu. Rev. Fluid Mech. **24**, 395 (1992).
[6] W. J. Staszewski and K. Worden, Int. J. Bifurcation Chaos Appl. Sci. Eng. **9**, 455 (1999).
[7] B. B. Mandelbrot and J. R. Wallis, Water Resour. Res. **4**, 909 (1968).
[8] B. B. Mandelbrot and J. R. Wallis, Water Resour. Res. **5**, 228 (1969).
[9] G. Wang, G. Antar, and P. Devynck, Phys. Plasmas **7**, 1181 (2000).
[10] M. Gilmore, C. X. Yu, T. L. Rhodes, and W. A. Peebles, Phys. Plasmas **9**, 1312 (2002).
[11] J. Beran, *Statistics for Long-Memory Processes* (Chapman & Hall, New York, 1994), pp. 50–53.
[12] G. Wornell, *Signal Processing With Fractals: A Wavelet-Based Approach* (Prentice-Hall, Upper Saddle River, 1996).
[13] E. Perrin, R. Harba, I. Iribarren, and R. Jennane, IEEE Trans. Signal Process. **53**, 1211 (2005).
[14] P. Abry and F. Sellan, Appl. Comput. Harmon. Anal. **3**, 377 (1996).
[15] D. B. Percival and A. T. Walden, *Wavelet Methods for Time Series Analysis* (Cambridge University Press, New York, 2000), pp. 257–287, 340–345, 457–500.
[16] P. Flandrin, IEEE Trans. Inf. Theory **35**, 197 (1989).
[17] P. Flandrin, in *Signal Processing V: Theories and Applications*, edited by L. Torres, E. Masgrau, and M. A. Lagunas (Elsevier, New York, 1990), pp. 149–152.
[18] M. J. Cannon, D. B. Percival, D. C. Caccia, G. M. Raymond, and J. B. Bassingthwaighte, Physica A **241**, 606 (1997).
[19] P. Flandrin, IEEE Trans. Inf. Theory **38**, 910 (1992).
[20] E. Masry, IEEE Trans. Inf. Theory **39**, 260 (1993).
[21] A. H. Tewfik and M. Kim, IEEE Trans. Inf. Theory **38**, 904 (1992).
[22] J. Beran, Stat. Sci. **7**, 404 (1992).
[23] H. P. Graf, Ph.D. thesis, ETH, Zurich, Switzerland (1983).
[24] M. S. Taqqu, Stochastic Proc. Appl. **7**, 55 (1978).
[25] M. S. Taqqu, in *Dependence in Probability and Statistics*, edited by E. Eberlin and M. S. Taqqu (Birkhauser, Boston, 1986), pp. 137–162.
[26] S. Mallat, *A Wavelet Tour of Signal Processing* (Academic, San Diego, 1998), pp. 82–83.
[27] S. Mallat, IEEE Trans. Pattern Anal. Mach. Intell. **2**, 674 (1989).
[28] D. Veitch and P. Abry, IEEE Trans. Circuits Syst., I: Fundam. Theory Appl. **45**, 878 (1999).
[29] J. Stöckel, J. Badalec, and I. Duran, Plasma Phys. Controlled Fusion **41**, A577 (1999).
[30] P. Devynck, G. Bonhomme, and E. Martines, Plasma Phys. Controlled Fusion **47**, 269 (2005).
[31] N. E. Huang, Z. Shen, S. R. Long, M. C. Wu, H. H. Shih, Q. Zheng, N.-C. Yen, C. C. Tung, and H. H. Liu, Proc. R. Soc. London, Ser. A **454**, 903 (1998).

Downloaded 08 Nov 2008 to 194.214.217.17. Redistribution subject to ASCE license or copyright; see http://pop.aip.org/pop/copyright.jsp